BIFURCATIONS AND CHAOS IN AUTOMATIC CONTROL SYSTEMS

Łukasz Kocewiak

Warsaw University of Technology,
Department of Electrical Engineering,
Pl. Politechniki, 00-661 Warsaw,
Poland

lukasz.kocewiak@gmail.com(Łukasz Kocewiak)

Abstract

The dynamics of power electronic system with pulse width modulation (PWM) control is studied in this paper. Behaviour characteristic for a nonlinear dynamical system is observed and theoretically explained. The set of system parameters influenced on periodic and chaotic oscillations existence are established and presented. For periodic motions, the regularities of their origin are studied and their possible bifurcations are established. A DC-DC buck converter controlled by a voltage feedback is taken as a representative system. The studied system is described by a system of piecewise-smooth nonautonomous differential equations. The research are focused on chaotic oscillations analysis and analytical search for bifurcations dependent on parameter. The most frequent route to chaos by the period doubling is observed in the second order DC-DC buck converter. Other bifurcations as a complex behaviour in power electronic system evidence are also described. The system sensitive dependence to initial conditions variation is studied and a positive largest Lyapunov exponent as a chaos indicator calculated. Appropriate methods of analysis are applied and used to observe chaotic phenomena. In order to verify theoretical investigation the experimental DC-DC buck converter was build. The results were obtained from three sources: mathematical model numerical calculation, electrical circuit computer simulation and experimental verification from the practical buck converter circuit. A very good agreement between theory and experiment was reached.

Keywords: Bifurcations, Chaos, Buck, Converter.

Presenting Author's Biography

Łukasz Kocewiak was born in Grójec, Poland, in 1983. He studies Electrical Engineering at Warsaw University of Technology. Within the confines of Socrates-Erasmus Programme he is a student of Department of Energy Technology at Aalborg University.
The main direction of his research is related with nonlinear dynamics in power electronics. Issues from scope of measurement and identification of power quality, identification and system parameter estimation, power electronics and drive and digital signal processing are also connected with his specialisation.

ISBN 978-3-901608-32-2

1 Introduction

The dynamics of DC-DC buck system is studied. System of this type have a broad range of applications for power control because of its high power efficiency and multiple direct current (DC) levels. Examples are power supplies for radio-electronics, computer equipment or spacecrafts [1, 7].

Ordinary differential equations with discontinuous right-hand sides constitute an important class of dynamical systems which applications to different problems in science and technology are variety and common (e.g. power electronics). On the basis of an example of a buck converter with a pulse width modulation (PWM) controller there will be determined the regions of periodic and chaotic oscillations. The regularities in the occurrence of periodic motions will be studied, and the associated bifurcations described.

There are two main reasons for studying chaotic circuits. It is important to know when and how this sort of behaviour can be present in an experimental situation, and if there is any to avoid it. From a more optimistic point of view, if a mode of operation is well understood, it can be useful in engineering. The understanding of chaotic behaviour in system operating modes can help to optimise a design process.

2 System description

The experimental example is a DC-DC buck converter[2, 6] which output voltage is controlled by a PWM with constant frequency, working in continuous conduction mode (CCM). A operation which is known as CCM, exists when a inductor current is never zero. The switches are assumed to be ideal.

In practise it is necessary to regulate low-pass filter output voltage v against changes in a input voltage and a load current, by adding a feedback control loop as in Fig. 1. In this proportional controller, a constant reference voltage V_{ref} is subtracted from the output voltage and the error, is amplified with gain A to form a control signal, $v_{co} = A(v - V_{ref})$. This signal feeds a PWM circuit comprising a ramp (sawtooth) generator of frequency f_s and voltage v_{ramp}. Switch driven by comparator conducts whenever $v_{co} < v_{ramp}$. The intended mode of operation is a steady state in which the output voltage stays close to V_{ref}.

The switched operation of converters implies a multi-topological model in which one particular circuit topology describes the system for a particular interval of time. Also, the operation is cyclic, implying that the involving topologies repeat themselves periodically. Thus, a natural way to model such kind of operation is to split the system into several subsystems, each being responsible for describing the system in one subinterval of time.

Considering that the linear amplifier has gain A, one can write

$$v_{co}(t) = A\Big(v(t) - V_{ref}\Big). \tag{1}$$

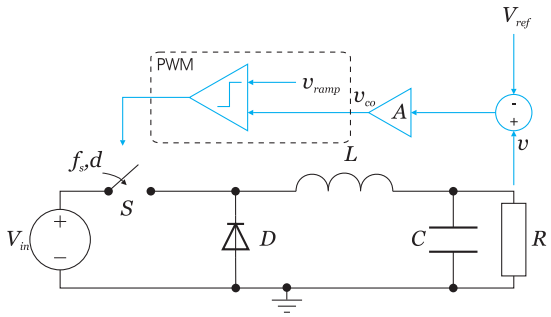

Fig. 1 Buck converter with proportional closed loop controller

Then, both control signal v_{co} and ramp voltage v_{ramp} are applied to the comparator, and every time the output difference changes its sign, the position of the switches S is commuted in such a way that S is open when the control voltage exceeds the ramp voltage. Otherwise S is closed.

Due to the fact that the discontinuous conduction mode does not take place, the converter can be represented by a piecewise linear vector field, described by two systems of differential equations as follows:

System I: $v_{co} \geq v_{ramp}(t)$

$$\frac{d}{dt}\begin{bmatrix} v(t) \\ i(t) \end{bmatrix} = \begin{bmatrix} -1/(RC) & 1/C \\ -1/L & 0 \end{bmatrix}\begin{bmatrix} v(t) \\ i(t) \end{bmatrix} \tag{2}$$

System II: $v_{co} < v_{ramp}(t)$

$$\frac{d}{dt}\begin{bmatrix} v(t) \\ i(t) \end{bmatrix} = \begin{bmatrix} -1/(RC) & 1/C \\ -1/L & 0 \end{bmatrix}\begin{bmatrix} v(t) \\ i(t) \end{bmatrix} + \tag{3}$$

$$+\begin{bmatrix} 0 \\ 1/L \end{bmatrix} V_{in}$$

where v is the capacitor voltage and i is the inductor current. Using the notation $\mathbf{x} = [v, i]^T$, ($\mathbf{y}^T$ donates the transpose of $\mathbf{y}$), (2) and (3) can be combined in only one expression

$$\frac{d\mathbf{x}}{dt} = \mathbf{f}(\mathbf{x}, t) \tag{4}$$

$$\mathbf{f}(\mathbf{x}, t) = \begin{bmatrix} -1/(RC) & 1/C \\ -1/L & 0 \end{bmatrix}\mathbf{x}(t) + \tag{5}$$

$$+\begin{bmatrix} 0 \\ V_{in}/L \end{bmatrix}\mathbf{1}_s(t).$$

where

$$\mathbf{1}_s(t) = \begin{cases} 0 & \text{if } t \notin s \\ 1 & \text{if } t \in s \end{cases} \tag{6}$$

ISBN 978-3-901608-32-2

and

$$s = \{t \geq 0 : v_{co} < v_{ramp}(t)\}.$$

And the ramp voltage is given by

$$v_{ramp}(t) = V_l + (V_u - V_l)t/T$$

where V_l and V_u are respectively the lower and upper voltages of the ramp and T its period.

3 Methods of theoretical analysis

The nonlinear phenomena includes bifurcations (sudden changes in operating mode), coexisting attractors (alternative stable operating modes), and chaos. If power converter is going to be designed, a knowledge about these issues existence and its investigation methods is vital. Unfortunately, popular analysis includes in most cases linear methods. Linear methods applied alone cannot give a wide spectrum of information of nonlinear phenomena and are insufficient in model predicting and analysing.

3.1 Largest Lyapunov Exponent

The usual test for chaos is calculation of the largest Lyapunov exponent (LLE) [13]. A positive LLE indicates chaos. When one has access to the equations generating chaos, this is relatively easy to do. The general idea is to follow two nearby orbits and to calculate their average logarithmic rate of separation. Infinite time Lyapunov exponents are suitable for characterising global behaviour of a system.

For most purposes, only the maximum Lyapunov exponent (LE) is considered. And it determines how sensitive a system is to initial conditions. Generally this is expressed in the limit as time goes to infinity, and can be written numerically as

$$\lambda_{max} = \lim_{t\to\infty} \frac{\ln\left(\frac{d(t)}{d_0}\right)}{t} \tag{7}$$

where $d(t)$ is the separation between the trajectories at time t, and d_0 is their separation at time zero, initial state.

Equation (7) is not directly usable because the system under consideration tends to be bounded and the rate of separation of trajectories is different in different regions of the phase space. If the trajectories at the beginning of evolution process are separated too much they will move into different regions, and further separation does not truly indicate the expansion rate around either trajectory.

Any method that is used for measuring the infinite time LE must either avoid these problems or must somehow keep the trajectories together (e.g. using renormalisation). Consider a particle placed on the trajectory of interest, $\mathbf{x}(t)$, while another particle is placed in some distance, d_0, away at $\mathbf{y}(t)$. The particles are evolved in time until some designated event occurs. At that time, to prevent the second particle from moving too far from the first, it is brought back towards the first to their initial separation, d_0. Using this method, the value of the Lyapunov exponent after the l-th renormalisation is [14]

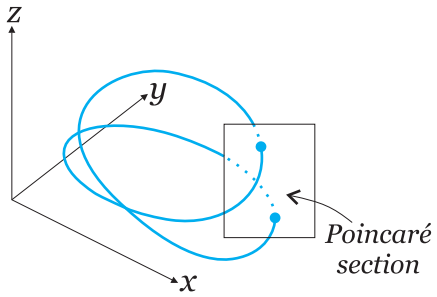

Fig. 2 Poincaré section (map) of limit cycle in the Poincaré plane (cross-section)

$$\lambda_l = \frac{1}{t_l}\sum_{k=1}^{l} \ln\frac{d(t_k)}{d_0} \tag{8}$$

where $d(t_k)$ is the separation between the particles before the k-th renormalisation. This value is equal to the true Lyapunov exponent when

$$d(t) \approx d_0^{1-l}\prod_{k=1}^{l} d(t_k) \tag{9}$$

If one is interested in all LEs, not just the largest, the more complex procedure of reorthonormalisation is needed.

3.2 Poincaré map

There are many cases where discrete-time dynamical systems (maps) naturally appear in the study of continuous-time dynamical systems defined by differential equations. The application of such maps in power electronic systems analysis allows to observe such nonlinear phenomena as bifurcations or chaos.

Before Poincaré will be defined consider a continuous-time dynamical system defined by

$$\dot{\mathbf{x}} = \mathbf{f}(\mathbf{x}), \qquad \mathbf{x} \in \mathbb{R}^n, \tag{10}$$

Assume, that (10) has a periodic orbit L_0. Take a point $\mathbf{x}_0 \in L_0$ and introduce a cross-section Σ to the cycle at this point. The cross-section Σ is a smooth hypersurface of dimension $n-1$, intersecting L_0 at a nonzero angle. The simplest choice of Σ is a hyperplane orthogonal to the cycle L_0 at $\mathbf{x}_0$.

Consider now orbits of (10) near the cycle L_0. The cycle itself is an orbit that starts at a point on Σ and returns to Σ at the same point. An orbit starting at a point $\mathbf{x} \in \Sigma$ sufficiently close to $\mathbf{x}_0$ also returns to Σ at some point $\tilde{\mathbf{x}} \in \Sigma$ near $\mathbf{x}_0$. Moreover, nearby orbits will also intersect Σ transversely. Thus, a map $P : \Sigma \to \Sigma$,

$$\mathbf{x} \to \tilde{\mathbf{x}} = P(\mathbf{x}),$$

is constructed. The map P is called a Poincaré map associated with the cycle L_0.

ISBN 978-3-901608-32-2

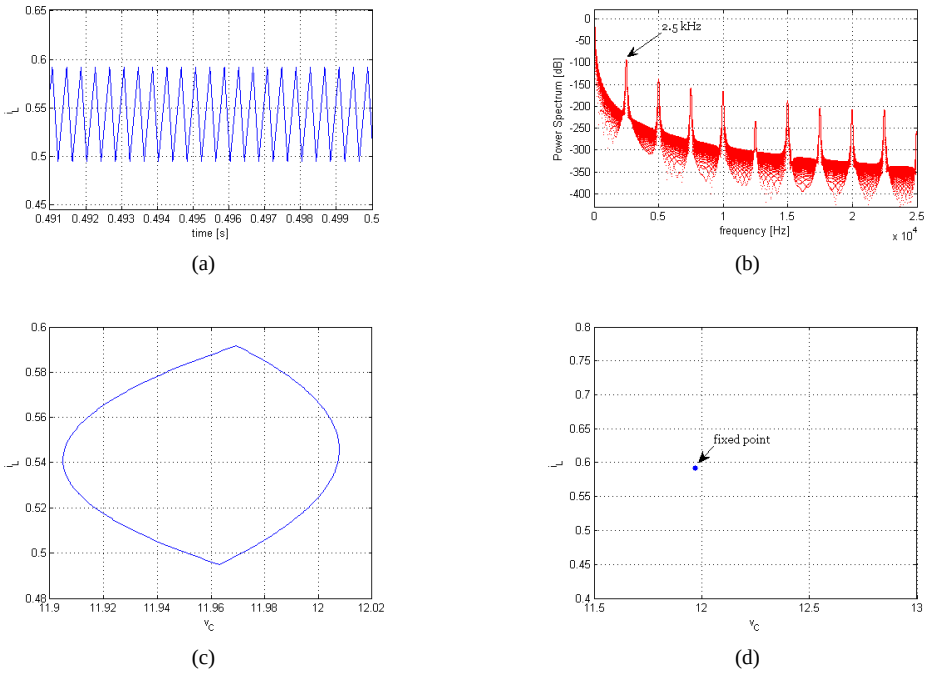

(a) (b) (c) (d)

Fig. 3 1T-periodic system operating mode (a) inductor current waveform (b) current power spectrum density (c) phase space trajectory of inductor current against a capacitor voltage (d) Poincaré section included one fixed point

Let introduce local coordinates $\xi = (\xi_1, \xi_2, \ldots, \xi_{n-1})$ on Σ such that $\xi = 0$ corresponds to $\mathbf{x}_0$. Then the Poincaré map will be characterised by a locally defined map $P : \mathbb{R}^{n-1} \rightarrow \mathbb{R}^{n-1}$,which transforms ξ corresponding to $\mathbf{x}$ into $\tilde{\xi}$ corresponding to $\tilde{\mathbf{x}}$,

$$P(\xi) = \tilde{\xi}$$

The origin $\xi = 0$ of $\mathbb{R}^{n-1}$ is a fixed point of the map P : $P(0) = 0$. The stability of the cycle L_0 is equivalent to the stability of the fixed point $\xi_0 = 0$ of the Poincaré map. Thus, the cycle is stable if all eigenvalues (multipliers) $\mu_1, \mu_2, \ldots, \mu_{n-1}$ of the $(n-1) \times (n-1)$ Jacobian matrix of P,

$$J_P = \left. \frac{dP}{d\xi} \right|_{\xi=0}$$

are located inside the unit circle $|\mu| = 1$

3.2.1 Poincaré map for periodically forced systems

In several applications the behaviour of a system subjected to an external periodic forcing is described by time-periodic differential equations

$$\dot{\mathbf{x}} = \mathbf{f}(\mathbf{x}, t), \qquad (\mathbf{x}, t) \in \mathbb{R}^n \times \mathbb{R}^1, \qquad (11)$$

where $\mathbf{f}(\mathbf{x}, t + T_0) = \mathbf{f}(\mathbf{x}, t)$. System (11) defines an autonomous system on the cylindrical manifold $X = \mathbb{S}^1 \times \mathbb{R}^n$, with coordinates $(\mathbf{x}, t(mod\ T_0))$, namely

$$\begin{cases} \dot{t} &= 1, \\ \dot{\mathbf{x}} &= \mathbf{f}(\mathbf{x}, t). \end{cases} \qquad (12)$$

In this space X, consider the n-dimensional cross-section $\Sigma = \{(\mathbf{x}, t) \in X : t = 0\}$ and $\mathbf{x} = [x_1, x_2, \ldots, x_n]^T$ are coordinates on Σ. Clearly, all orbits of (12) intersect Σ transversely. Assuming that the solution $\mathbf{x}(\mathbf{x}_0, t)$ of (12) exists on the interval $t \in [0, T_0]$, introduce the Poincaré map

$$\mathbf{x}_0 \mapsto P(\mathbf{x}_0) = \mathbf{x}(\mathbf{x}_0, T_0). \qquad (13)$$

In other words, one has to take an initial point $\mathbf{x}_0$ and integrate system over its period T_0 to obtain $P(\mathbf{x}_0)$. By this construction, the discrete-time dynamical system is defined.

The advantage of using cylindrical space to present the solution of the system is that there is a possibility to observe the evolution of the state of the system, $\mathbf{x}(t)$, as a function of time $t \in [0, T_0]$, and easily visualise the possible periodic orbits.

The basic problem with this attitude refers to the choice of the appropriate sampling frequency. For non-autonomous systems like in analysed DC-DC buck converter, the driving frequency is a proper choice if any periodic behaviour of the system is related to the driving frequency. For switching converters, the switching frequency is the natural choice. However, this sampled-data method is in principle not suitable for autonomous systems which do not possess any externally driven periodic source.

3.3 Bifurcations

There are two broad classes of transitions to chaos: the local and global bifurcations. In the first case one limit

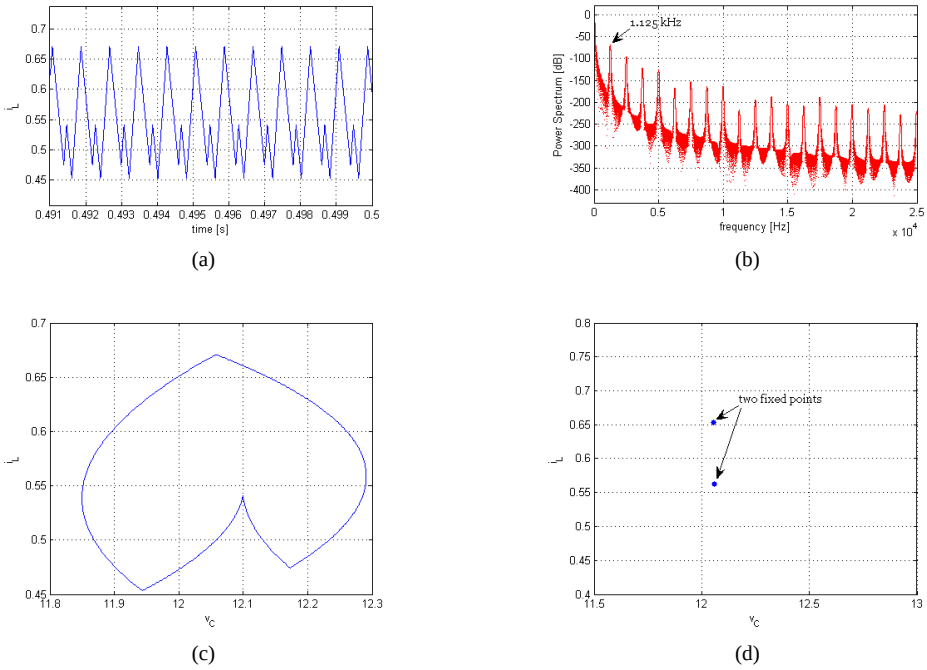

(a) (b) (c) (d)

Fig. 4 2T-periodic system operating mode (a) inductor current waveform (b) current power spectrum density (c) phase space trajectory of inductor current against a capacitor voltage (d) Poincaré section included two fixed points

cycle or fixed point loses its stability. The local bifurcation has three subclasses: period doubling, quasi-periodicity and intermittency. The most frequent route is the period doubling also present in the DC-DC buck converter. In the global bifurcation more fixed points and/or limit cycles lose its stability. It has two subdivisions, the chaotic transient and the crisis.

In the study of dynamical systems in the form of differential equations, a bifurcation occurs when a small smooth change made to the parameter values (the bifurcation parameters) of a system causes a sudden qualitative change in the system's long-term dynamical behaviour [10].

The appearance of a topologically nonequivalent phase portrait under variation of parameters is called a bifurcation. Thus, a bifurcation is a change of the topological type of the system as its parameters pass through a bifurcation (critical) value.

Consider a continuous-time system that depends smoothly on a parameter:

$$\dot{\mathbf{x}} = \mathbf{f}(\mathbf{x}, \alpha), \qquad \mathbf{x} \in \mathbb{R}^n,\ \alpha \in \mathbb{R}^1. \qquad (14)$$

Let L_0 (see Fig. 5) be a limit cycle of system (14) at $\alpha = 0$. Let P_α denote the associated Poincaré map for nearby α; $P_\alpha : \Sigma \to \Sigma$,where Σ is a local cross-section to L_0. If some coordinates $\xi = (\xi_1, \xi_2, \ldots, \xi_{n-1})$ are introduced on Σ,then $\tilde{\xi} = P_\alpha(\xi)$ can be defined to be the point of the next intersection with Σ of the orbit of (14) having initial point with coordinates ξ on Σ. The intersection of Σ and L_0 gives a fixed point ξ_0 for P_0 : $P_0(\xi_0) = \xi_0$.

Suppose that at $\alpha = 0$ the cycle has a simple multiplier $\mu_1 = -1$, while $-1 < \mu_2 < 0$. Then, the restriction of P_α to the invariant manifold will demonstrate generically the period-doubling (flip) bifurcation: A cycle of period two appears for the map, while the fixed point changes its stability. Since the manifold is attracting, the stable fixed point, for example, loses stability and becomes a saddle point, while a stable cycle of period two appears. The fixed points correspond to limit cycles of the relevant stability. The cycle of period-two points for the map corresponds to a unique stable limit cycle.

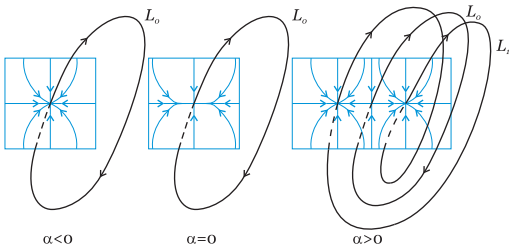

Fig. 5 Flip bifurcation of limit cycle

3.3.1 Period doubling bifurcation

If an iterative map is used to model the system, the linearised system needs to be examined. Suppose the iter-

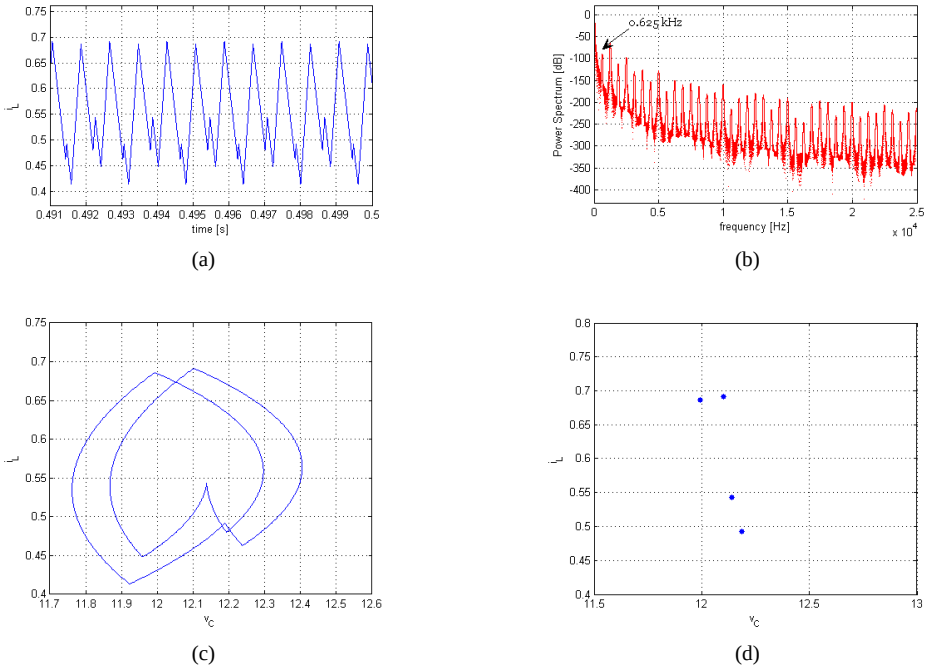

Fig. 6 4T-periodic system operating mode (a) inductor current waveform (b) current power spectrum density (c) phase space trajectory of inductor current against a capacitor voltage (d) Poincaré section

ative map is

$$\mathbf{x} \mapsto \mathbf{f}(\mathbf{x}, \alpha) \qquad \mathbf{x} \in \mathbb{R}^n,\ \alpha \in \mathbb{R}^1,$$

then the Jacobian $J_f = \partial \mathbf{f}/\partial \mathbf{x}^T$ characterising the linearised system is given by evaluated at the fixed point. The eigenvalues of system can be obtained by solving the characteristic equation

$$det(\mu \mathbf{1} - J_f) = 0$$

In this case, the modulus of the eigenvalues needs to be taken into account. If one of the eigenvalues is observed to move out of the unit circle on the real line, through the point -1, then we may establish a period doubling. Generally, the bifurcation associated with the appearance of $\mu_1 = -1$ is called a period-doubling (or flip) bifurcation.

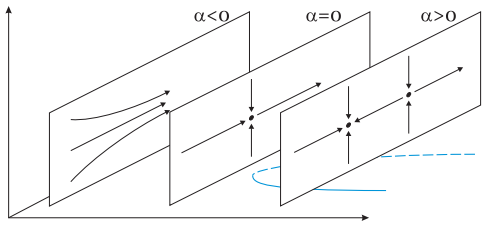

Fig. 7 A fixed point appears at parameter $\alpha = 0$ in a saddle-node bifurcation. For $\alpha > 0$ there is an attracting fixed point and a saddle fixed point. The cross-sectional figures depict the action of the planar map at that parameter value.

Periodic orbits of periods greater than one can come into (or go out of) existence through saddle-node bifurcations, and they can undergo period-doubling bifurcations (see Fig. 7). This kind of behaviour exists in analysed DC-DC buck converter and it will be shown below.

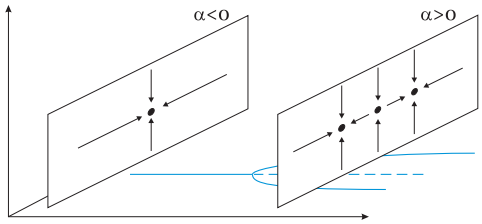

Fig. 8 An attracting fixed point loses stability at $\alpha = 0$ in a period-doubling bifurcation. For $a > 0$ there is a saddle fixed point and a period-two attractor.

At a period-doubling bifurcation from a period-k orbit (see Fig. 8), two branches of period-$2k$ points emanate from a path of period-k points. When the branches split off, the period-k points change stability (going from attractor to repeller, or vice versa).

4 Computer simulation

Assuming the notation of from used in previous sections, the parameters of the circuit are: R, C, and L, the resistance, the capacitance and the inductance of the circuit respectively; V_l and V_u, the lower and upper voltages of the ramp and T, its period equals $\frac{1}{f}$; A, the

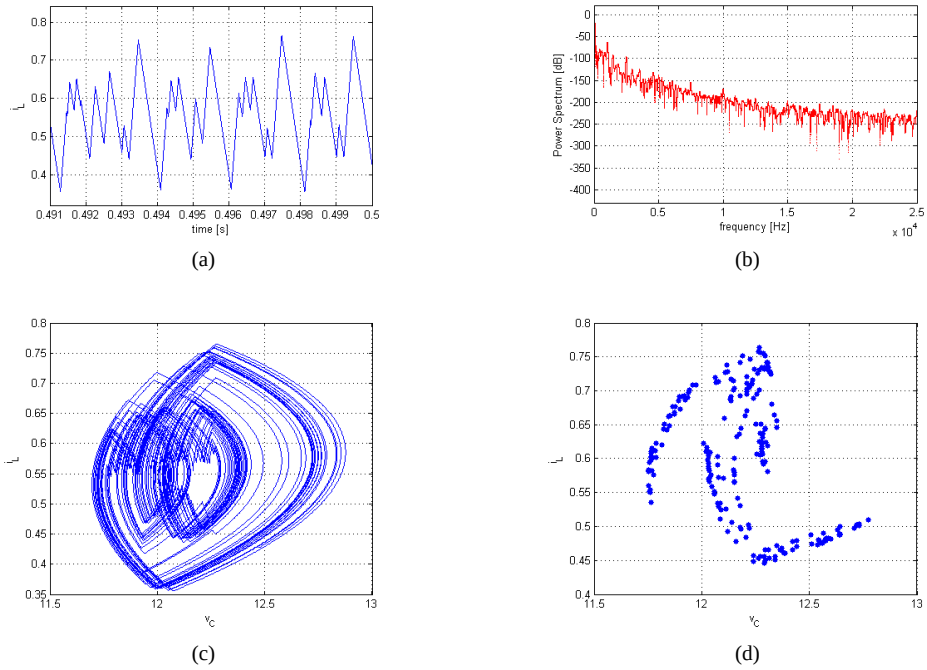

Fig. 9 Chaotic system operating mode (a) inductor current waveform (b) current power spectrum density (c) phase space trajectory of inductor current against a capacitor voltage (d) Poincaré section

gain of the amplifier; V_{ref}, the reference voltage, and V_{in}, the input voltage. The buck converter is investigated using the following parameter values: L=20 mH, C=47 μF, R=22 Ω, A=8.2, V_{ref}=11.3 V, V_l=3.8 V, V_u=8.2 V, ramp frequency f=2.5 kHz [3, 6]. There was investigated the variations of $V_{in} \in$[20 V,35 V] as the bifurcation parameter. The integration has been performed based on `ode23tb` Matlab-provided algorithm with variable step size.

4.1 Theoretical model simulation

One of the routes to chaos is by period doubling, which continues until there are no further stable states available. At the beginning of simulation when input voltage is 20 V circuit exhibits periodic behaviour. During system bifurcation parameter (V_{in} - input voltage) changes, periodic state becomes unstable because of flip bifurcation.

In spectral analysis presented in Fig.3(b) it is observed as second frequency appearing at half the driving frequency. Further increase in input voltage results in splitting of two periods (see Fig.4(b)), giving quadrupling (Fig.6(b)), octupling and finally chaos in Fig.9(b). This is called the period doubling cascade route to chaos.

LLEs plotted against bifurcation parameter are presented in Fig. 10. As one can see LLE approximately equals 0 when limit cycle is considered no matter how complex. Near the last period-doubling bifurcation, suddenly and at approximately 32.4 V , there is a large chaotic behaviour. And LLE as a qualitative indicator of chaos is positive. Further input voltage increasing shows chaotic oscillations all the time.

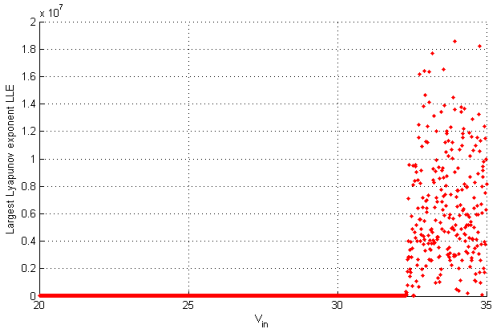

Fig. 10 Largest Lyapunov exponent calculated using difference method

The parametric portrait together with its characteristic phase portraits constitute a bifurcation diagram. A bifurcation diagram of the dynamical system is a stratification of its parameter space together with representative phase portraits for each stratum. It is desirable to obtain the bifurcation diagram as a result of the qualitative analysis of a given dynamical system. It classifies in a very condensed way all possible modes of behaviour of the system and transitions between them (bifurcations) under parameter variations.

Because it is easy to vary, the input voltage V_{in} was chosen as the bifurcation parameter. The i_L, v_C and v_{co} were sampled at the start of every ramp cycle and plotted as the bifurcation diagram as it is shown in Fig.11. A period doubling route to chaos is visible. This pro-

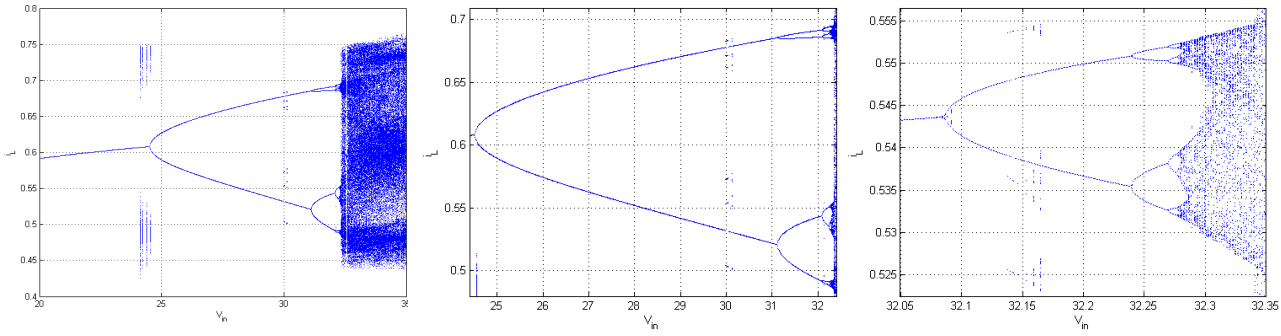

(a) (b) (c)

Fig. 11 Bifurcation diagram with V_{in} as the bifurcation parameter

cess is repeated for every discrete value of the bifurcation parameter in the interval $V_{in} \in [20, 35]$ V.

There was computed that stable 1T-periodic orbit (limit cycle) is initially found (see Fig. 3) and continued until some value near 24.5 V. Then, a first period-doubling bifurcation occurs, and the stability of the 1T-periodic orbit is lost in favour of the 2T-periodic orbit which appears at this value as it is shown in Fig. 4. This 2T-periodic orbit also loses stability in a period-doubling bifurcation near 31.15 V shown in Fig. 6. The unstable orbits cannot appear in a bifurcation diagram what was shown in Fig. 11. Near the last period-doubling bifurcation, suddenly and at approximately 32.4 V , there is a large chaotic behaviour, as can be seen in Fig. 9.

Parallel branches of 6T-periodic orbit are detected in a neighbourhood of V_{in}=30.000 V which is shown in Fig. 11. This undergoes its own period-doubling cascade which ends in a six-piece chaotic attractor coexisting with the main 2T-periodic stable orbit. A further branch of 12T-periodic orbit is found in a neighbourhood of V_{in}=32.15 V (see Fig. 11) and born after a saddle-node bifurcation and coexisting with the 8T-periodic stable orbit generated at the third period-doubling of the 1T-periodic main orbit, which gives rise to a twelve-piece chaotic attractor via a period-doubling cascade once again.

The Poincaré section diagram (see Fig. 3(d), 4(d), 6(d), 9(d)) come into being as a result of simulated waveforms sampling synchronised with the ramp voltage, one sample of the current and voltage variables at the beginning of the ramp. Then the representation in the state space of the points obtained with this procedure gives the discrete evolution of the system. For periodically driven (non-autonomous) systems, like most of the fixed frequency switching converters, information about periodicity can be easily obtained by sampling the waveforms. Essentially, one take a waveform from computer simulation in this case, extract its value at periodic time instants equals ramp signal period and look for specific patterns.

4.2 Electrical circuit computer simulation

In order to compare mathematical model and designed circuit, PSpice simulation has been carried out before DC-DC buck converter laboratory realisation.

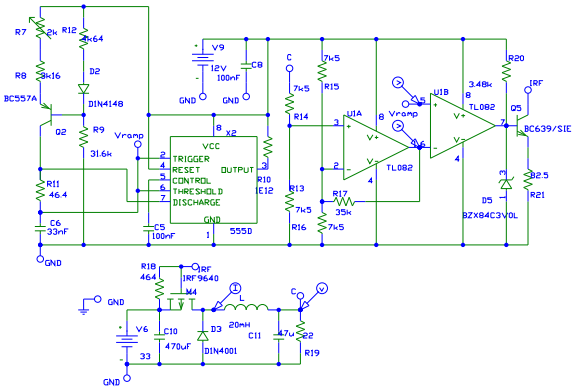

Fig. 12 Circuit diagram of the experimental buck converter

The power circuit (see. Fig.12) uses a power metal-oxide-semiconductor field-effect transistor (MOSFET) IRF9640 and power standard recovery diode 1N4001. The DC input voltage has been varied from 20 to 35 V, control circuit have been supplied from a stable +12 V rail. The ramp generator, based on a 555 timer, produces a sawtooth waveform. Wide band dual operational amplifier TL082 is used as a comparator and a difference amplifier. Comparator is fed by sawtooth waveform and difference amplifier that takes the difference between v and V_{ref} derived from the +12 stabilised rail.

The values of circuit components give approximately similar system as previously simulated: L =20 mH, C =47 μF, R =22 Ω, T =400 μs, V_l =3.8 V, V_u =8 V and V_{ref} =12 V. There has been carried out the simulation of designed circuit before physical realisation.

ISBN 978-3-901608-32-2

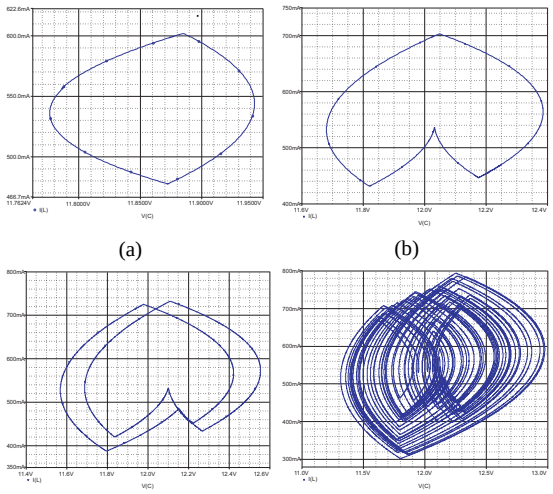

(a) (b)

(c) (d)

Fig. 13 Phase space trajectory obtained from PSpice (a) 1T periodic orbit (b) 2T periodic orbit (c) 4T periodic orbit (d) chaotic orbit

The results of simulation using PSpice are comparable to simulated mathematical model and presented in Fig. 13. It is the strong evidence of circuit designing correctness. Phase space trajectory changes as a result of period doubling bifurcation are clearly shown.

5 Practical verification

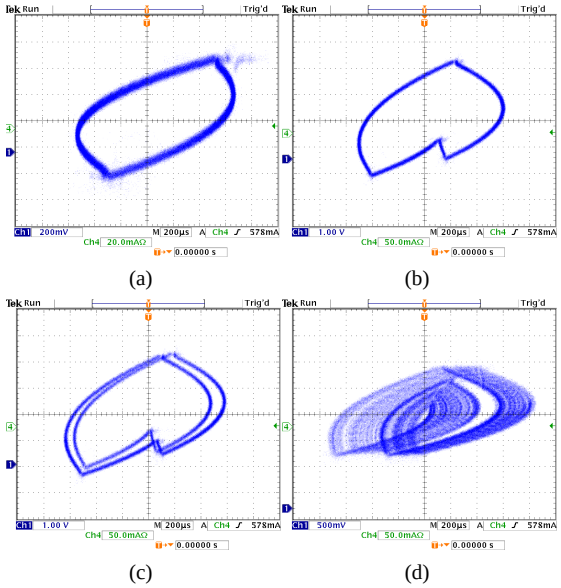

(a) (b)

(c) (d)

Fig. 14 Phase space trajectory measured in a laboratory (a) 1T periodic orbit (b) 2T periodic orbit (c) 4T periodic orbit (d) chaotic orbit

The power circuit uses a power MOSFET IRF9640 and a Schottky diode. Probably the greatest deviation from theoretical model poses the coil series resistance not included in the mathematical equations and equals 0.3 Ω. The DC input voltage from 20 to 35 V is passed through a positive voltage regulator LM7812 that provides a stable +12 V rail for the control circuit. The ramp generator, based on a LM555 timer, produces an accurate sawtooth waveform. As the comparator is applied LM311 and as the difference amplifier is used a complementary metal-oxide-semiconductor (CMOS) operational amplifier LMC662. Comparator is fed by a sawtooth waveform and a difference amplifier that takes the difference between v and V_{ref} derived from a +12 stabilised rail.

The results from the laboratory experiment are similar to the simulations from PSpice and from Matlab and are presented in Fig. 14. As is able to observe the qualitative character of all results is the same. Every time bifurcations and chaotic oscillations are presented.

6 Results comparison

In order to verify obtained results there will be a breakdown presented. The outcomes of mathematical model from Matlab in comparison with the results from PSpice simulated circuit and the physical laboratory experiment will be shown.

The results were obtained from three sources:

1. Numerical calculations from Matlab. There was the mathematical model simulated.
2. Simulation using PSpice, with consideration of additional effects present in practical realisation (non-ideal elements).
3. Experimental results from the practical buck converter circuit.

The 4T-orbit (limit cycle) has been chosen for the sake of sufficient complexity and is presented in Fig.15. Such a presentation enables clear observation of behaviour present in the system. This attractor appears after second flip bifurcation and is a premise of chaotic phenomena existed in the DC-DC second-order buck converter with the voltage control.

7 Conclusion

The main objective was to present nonlinear system analysing methods and its application in power electronics. The DC-DC second-order buck converter with the voltage control was taken as an example. The main aim was to build a converter which is able to work in chaotic operating mode basis of the mathematical model. Simultaneously there were shown analytical methods helpful in detecting, analysing and classifying this kind of nonlinear behaviour.

Additionally it was presented that nonlinear analysis describes analysed system more accurately and explains phenomenons (e.g. subharmonics, bifurcations and chaos), which cannot be detected by using linear approach of analysis. It proves that it could be useful in circuits study, specially in a field where high reliability is essential, like in spacecraft power systems or terrestrial power systems.

ISBN 978-3-901608-32-2

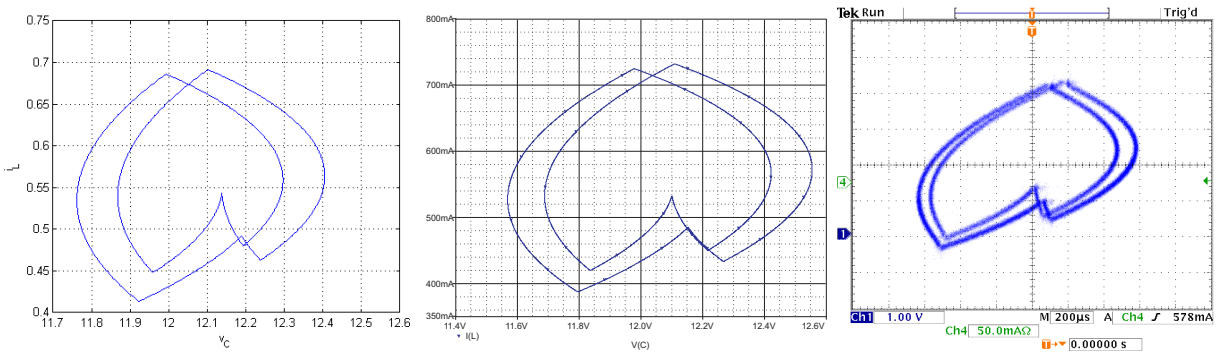

(a) (b) (c)

Fig. 15 4T periodic limit cycle comparison (a) 4T periodic orbit from Matlab (b) 4T periodic orbit from PSpice (c) 4T periodic orbit obtained in a laboratory

The investigation was carried out in three different ways and the results were compared. There were considered three independent cases: the mathematical model simulated in Matlab, the circuit builded from components exist in reality and simulated in PSpice and the laboratory experiment. All of cases give satisfactory results and they have been described in relevant sections.

8 Future work

The theory of chaos has been recently applied in engineering but at present there are a lot of analysis methods, which can be used in the DC-DC buck converter.

There is a possibility to find an application of following methods:

1. Several discrete-time maps have been defined to develop the analysis of nonlinear phenomena in DC-DC converters. Except for stroboscopic maps described in this paper there are also A-switching and S-switching ones. Application can provide more information about system and give more accurate system description.

2. Lyapunov exponents computation from short time-series. This method has a strong application in system analysis with unknown description and could be used directly in power electronics.

One cannot exclude the possibility of other forms of bifurcation that may occur in this class of switching converters. In future there is also a possibility to study the same converter controlled under a different scheme.

9 References

[1] Zh.T. Zhusubaliyev, E. Soukhoterin, E. Mosekilde. Quasiperiodicity and torus breakdown in a power electronic DC-DC converter. *Mathematics & Computers in Simulation*, 73:364-377, 2007.

[2] N. Mohan, T.M. Undeland, W.P. Robbins. *Power Electronics: Converters, Applications and Design*. John Wiley & Sons Inc., 2003.

[3] F. Angulo, C. Ocampo, G. Olivar, R. Ramos. Nonlinear and nonsmooth dynamics in a DC-DC buck converter: Two experimental set-ups. *Nonlinear Dynamics*, 46:239-257, 2006.

[4] J. Awrejcewicz, C.H. Lamarque. *Bifurcations and Chaos in Nonsmooth Mechanical Systems*. Word Scientific, London, 2003.

[5] Y. Guohui, S. Banerjee, E. Ott, J.A. Yorke. Border-collision bifurcations in the buck converter. *Circuits and Systems I: Fundamental Theory and Applications*, 45:707-716, 1998.

[6] D.C. Hamill, J.H.B. Deane, P.J. Aston. Some applications of chaos in power converters. *Update on New Power Electronic Techniques*, 23:1-5, 1997.

[7] Y.H. Lim, D.C. Hamill. Bifurcations and chaos in models of spacecraft power systems. *International Symposium on Nonlinear Theory and its Applications*, 1:335-338, 1998.

[8] D.C. Hamill, J.H.B. Deane, D.J. Jefferies. Modeling of chaotic dc-dc converters by iterated nonlinear mappings. *IEEE Trans. on Power Electronics*, 7:25-36, 1992.

[9] M.T. Rosenstein, J.J. Collins, C.J. De Luca. A practical method for calculating largest Lyapunov exponents from small data sets. *Physica D*, 65:117-134, 1993.

[10] Y.A. Kuznetsov. *Elements of applied bifurcation theory*. Springer-Verlag.

[11] Chi Kong Tse. *Complex Behaviour of Switching Power Converters*. CRC Press, 2000.

[12] D.G. Manolakis, V.K. Ingle, S.M. Kogon. *Statistical and Adaptive Signal Processing: Spectral Estimation, Signal Modelling, Adaptive Filtering and Array Processing*. McGraw-Hill, 2000.

[13] K. Alligood, T. Sauer, J.A. Yorke. *Chaos: An Introduction to Dynamic Systems*. Springer-Verlag, New York, 1996.

[14] G. Benettin, L. Galgani, A. Giorgilli, J.M. Strelcyn. Lyapunov characteristic exponents for smooth dynamical systems and for Hamiltonian systems; a method for computing all of them. Part 2: numerical application. *Meccanica*, 21-30, 1980.

ISBN 978-3-901608-32-2